POLITECNICO DI TORINO
Repository ISTITUZIONALE

Synthesis of bioinspired collagen/alginate/fibrin based hydrogels for soft tissue engineering

Original
Synthesis of bioinspired collagen/alginate/fibrin based hydrogels for soft tissue engineering / Montalbano, G., Toumpaniari, S., Popov, A., Duan, P., Chen, J., Dalgarno, K., Scott, W.E., Ferreira, A.M.. - In: MATERIALS SCIENCE AND ENGINEERING. C, BIOMIMETIC MATERIALS, SENSORS AND SYSTEMS. - ISSN 0928-4931. - ELETTRONICO. - 91:(2018), pp. 236-246. [10.1016/j.msec.2018.04.101]

Availability:
This version is available at: 11583/2732748 since: 2019-05-09T15:41:32Z

Publisher:
Elsevier Ltd

Published
DOI:10.1016/j.msec.2018.04.101

Terms of use:

This article is made available under terms and conditions as specified in the corresponding bibliographic description in the repository

Publisher copyright

(Article begins on next page)

13 September 2026

Materials Science & Engineering C 91 (2018) 236–246

Contents lists available at ScienceDirect

Materials Science & Engineering C

journal homepage: www.elsevier.com/locate/msec

Synthesis of bioinspired collagen/alginate/fibrin based hydrogels for soft tissue engineering

G. Montalbano[a,c,1], S. Toumpaniari[a,d,1], A. Popov[a,e,1], P. Duan[a], J. Chen[a], K. Dalgarno[a], W.E. Scott III[b], A.M. Ferreira[a,*]

[a] School of Engineering, Newcastle University, Newcastle Upon Tyne NE1 7RU, UK
[b] Institute of Cellular Medicine, Newcastle University, Newcastle Upon Tyne NE1 7RU, UK
[c] Department of Applied Science and Technology, Politecnico di Torino, Turin 10129, Italy
[d] Cambridge Centre for Medical Materials, University of Cambridge, Cambridge CB3 0FS, UK
[e] UCL Cancer Institute, University College London, London WC1E 6BT, UK

ARTICLE INFO

Keywords:
Hydrogels
Collagen
Alginate
Fibrin
Soft tissue engineering

ABSTRACT

Hydrogels based on natural polymers offer a range of properties to mimic the native extracellular matrix, and provide microenvironments to preserve cellular function and encourage tissue formation. A tri-component hydrogel using collagen, alginate and fibrin (CAF) was developed and investigated at three collagen concentrations for application as a functional extracellular matrix analogue. Physical-chemical characterization of CAF hydrogels demonstrated a thermo-responsive crosslinking capacity at physiological conditions with stiffness similar to native soft tissues. CAF hydrogels were also assessed for cytocompatibility using L929 murine fibroblasts, pancreatic MIN6 β-cells and human mesenchymal stem cells (hMSCs); and demonstrated good cell viability, proliferation and metabolic activity after 7 days of in vitro culture. CAF hydrogels, especially with 2.5% w/v collagen, increased alkaline phosphatase production in hMSCs indicating potential for the promotion of osteogenic activity. Moreover, CAF hydrogels also increased metabolic activity of MIN6 β-cells and promoted the reconstitution of spherical pseudoislets with sizes ranging between 50 and 150 μm at day 7, demonstrating potential in diabetic therapeutic applications.

1. Introduction

To date, biomaterials for regenerative medicine applications have primarily focused on controlling cell function and lineage commitment [1,2]. These materials can be tailored to provide a tissue-specific biomimetic microenvironment for cell housing and protection from hostile environment and immune-attack prior to engraftment; improving adhesion, viability and function. Hydrogels are hydrated biomaterials capable of suspending cells at targeted sites for cell engraftment [2,3], with control of permeability and mechanical properties possible through modulating the viscosity. Polymeric hydrogels have become attractive extracellular matrix (ECM) substitutes for biomedical applications due to their specific combination of biocompatibility, biodegradability, the "tunability" of mechanical properties, biomimicry, modularity, and responsiveness, as well as their innate ability to retain large amounts of water, promoting cell health [2,4,5]. For this reason, hydrogels based on natural polymers offer a versatile platform to engineer diverse combinations of properties to mimic features of native ECM and to provide spatial support and access to functional moieties such as RGD, to preserve cellular functions and encourage tissue formation [6–9]. Many of these materials are designed to be delivered using minimally invasive techniques, with the aim to create complex structures and organizations via extrusion processes involving catheters or syringes [10–12]. Versatile hydrogels allows to bioengineer 3D cell culture studies, including cellular organization into organoids and tissue formation ex vivo, for developing great new models for drug detection and tissue regeneration in the clinic [13,14].

Collagen is the main structural protein for most tissues and is able to self-assemble into fibril structures under physiological conditions. This makes it an ideal component in engineered tissues as it can impart mechanical properties to otherwise amorphous hydrogels; which can be modulated to mimic native tissues [15–17]. It provides ready access to several key recognition sites for cellular migration and attachment, as well as providing long-term structural support to tissues [18]. Alginate is a readily available natural biopolymer, which provides good long-time stability, can be purified to prevent immunogenicity [18], and is

* Corresponding author at: School of Engineering, Newcastle University, Claremont Road, Newcastle Upon Tyne NE1 7RU, UK.
E-mail address: ana.ferreira-duarte@ncl.ac.uk (A.M. Ferreira).
[1] These authors contributed equally to this work.

https://doi.org/10.1016/j.msec.2018.04.101
Received 11 September 2017; Received in revised form 13 March 2018; Accepted 28 April 2018
Available online 17 May 2018
0928-4931/ © 2018 The Authors. Published by Elsevier B.V. This is an open access article under the CC BY license (http://creativecommons.org/licenses/BY/4.0/).

able to absorb large amount of aqueous biological fluids [19,20]. Fibrin is also a native biopolymer, formed physiologically during blood coagulation, which has a critical role in haemostasis and tissue repair, stimulating wound healing and thus encouraging implant engraftment [21,22]. Like collagen, fibrin possesses several key amino acid binding sequences, including two pairs of RGD sites involved in cell-integrin interactions [21]. These materials can be tailored to provide a tissue-specific biomimetic microenvironment for cell housing, improving in situ retention and viability, while simultaneously providing protection from potentially hostile environments such as those found in injured or diseased tissues [5,23,24].

A variety hydrogels have been formulated by using these biopolymers and derivatives (i.e. alginate, gelatin, fibrin, collagen, etc.) as encapsulation systems, microfluidic hydrogels, injectable materials, cell delivery systems, scaffolds, and as bioink for biofabrication [25,26]. Alginate-fibrin hydrogels have demonstrated the ability to induce in vitro osteogenic differentiation of adipose stem cells [27]; enable fast release of stem-cells when used as a stem-cell encapsulation system [28]; support chondrogenesis of bone-derived mesenchymal stems cell [29]; and support in vitro development of caprine preantral follicles [30]. Similar hydrogels systems have also incorporated gelatin for fabricating tubular constructs similar to blood vessels [31], biomimetic scaffolds for cartilage regeneration [32], in vitro physiological models of the metabolic syndrome [25], and aortic valve conduits by 3D bioprinting [33]. Gelatin is the denaturated version of the collagen protein, thus several important biological and physical-chemical properties differ between the two biopolymers including gelation temperatures [34] and cellular binding mechanisms [35]. While various studies have shown the advantages and application of hydrogels combinations such as collagen-alginate [36–38], fibrinogen-alginate [29,39,40] and collagen-fibrinogen [41,42] hydrogels; the formulation of collagen-fibrinogen-alginate into a tri-component hydrogel, potentially combining the benefits of all three components, has not been explored before.

Here we describe the formulation and characterization of a new thermo-responsive hydrogel inspired by native ECM that integrates the excellent biological properties of collagen as an extracellular matrix structural protein, fibrin as a natural regulator of haemostasis and tissue repair, and alginate for controlled protein release. While collagen has been widely used as hydrogel for tissue engineering applications [43–48], the use of collagen combined with alginate and fibrin has not previously been investigated. A new synthesis scheme is described and was used to create three different collagen concentrations, which were characterized to determine physical-chemical properties and cellular response. Biological potential of formulated CAF hydrogels hold for soft tissue engineering applications, particularly musculoskeletal and pancreatic applications, is demonstrated by using three different cell types: murine fibroblasts (L929), murine pancreatic β-cells (MIN6) and human-TERT mesenchymal stem cells (Y201 hMSCs) [49].

2. Materials and methods

2.1. Materials

Type I collagen from calf skin (Sigma Aldrich, C9791-250MG), alginic acid sodium salt from brown algae - low viscosity (Sigma, A1112 – 100G), fibrinogen from bovine plasma (Sigma, F8630 - 1G), thrombin from bovine plasma (Sigma, T4648 – 1KU), (2%, v/v) acetic acid (Sigma Aldrich, A6283), NaOH (1 M), Dulbecco's Modified Eagle's Medium (Sigma, DMEM – 500 ML), Phosphate Buffered Saline (PBS) (Sigma Aldrich, PBS1).

2.2. Methods

2.2.1. Collagen-Alginate-Fibrin (CAF) hydrogel preparation

Collagen solutions were prepared at three concentrations, 0.5%, 1% and 2.5% w/v, by dissolving collagen powder in 2% v/v acetic acid at 4 °C. Once dissolved, the pH of the collagen solutions was adjusted to 5.5–6. A 5% alginate solution was prepared by dissolving alginic acid sodium salt powder in sterile calcium free PBS and pasteurized by incubation at 70 °C for 20 min and allowed to cool down to room temperature. This process was repeated three times. The solution was then slowly stirred until fully dispersed, to obtain a viscous solution. 10% w/v fibrinogen solution was obtained by dissolving fibrinogen powder in sterile PBS solution, and filtered using a 0.22 μm filter. Alginate and fibrinogen solutions were then mixed at a 1:1 ratio. Then, the collagen solution was added to the alginate/fibrinogen mixture so that a volume ratio of 2:1:1 (collagen solution: alginate solution: fibrin solution) was obtained, and the mixture stirred until homogenous. The pH of the CAF solution was then adjusted to 7.4. CAF hydrogels were then formed by polymerizing the single components in the mixture, as follows: 1) collagen gelation was induced by increasing the temperature to 37 °C in an incubator, until a self-contained gel is formed; then 2) alginic acid was polymerized by calcium diffusion through the gel by using 10% w/v of $CaCl_2$ in distilled water for 1 min; 3) the CAF gel was then incubated for 15 min in a 1 U/mL of thrombin solution prepared by dissolving thrombin powder in PBS containing 0.1% FBS in order to polymerize fibrinogen into fibrin. Before use the $CaCl_2$ and thrombin were filtered using a 0.22 μm filter.

2.3. Characterization methods

2.3.1. Attenuated Total Reflection Fourier Transform Infrared Spectroscopy (ATR-FTIR)

PerkinElmer UATR-Two, equipped with diamond total reflectance (ATR) crystal and PerkinElmer Spectrum Software analyse the chemical composition of freeze-dried hydrogels in the range of 550–4000 cm^{-1} at a resolution of 4 cm^{-1} and 32 scans.

2.3.2. Scanning Electron Microscopy (SEM)

Hydrogel samples were frozen in liquid nitrogen and freeze-dried using an ALPHA 1–2 LD plus freeze-dryer, at 0.060 mbar for 48 h. The CAF hydrogels were studied using a low vacuum SEM (Hitachi TM 3030), with an accelerating voltage of 15 kV. Pore sizes were measured from the SEM images (n = 4 samples) using ImageJ software (National Institutes of Health, USA).

2.3.3. Transmission electron microscopy (TEM)

Hydrogels samples were fixed overnight in 2.5% glutaraldehyde at 4 °C. Then, samples were post-fixed treated with 0.5% OsO_4. Images were obtained after samples were embedded in resin and sectioned, using a Philips CM100 Transmission EM at HV = 100.0 kV and a range of magnifications up to 130,000×.

2.3.4. Gelation time

The gelation time was assessed using the “vial tilt” method. Vials (n = 5) were filled with 1 mL of 0.5%, 1% and 2.5% CAF hydrogel and incubated at 37 °C. Samples were then tilted every 5 min and classified as either a solution or gel.

2.3.5. Equilibrium swelling

Freeze-dried hydrogels were immersed in sealed vials containing phosphate buffer saline (PBS). After 24 h of incubation, the samples were removed from the vials and weighed (W_w), removing any excess water with filter paper. The equilibrium swelling of each hydrogel was calculated from:

$$\text{Swelling}\,(\%) = [(W_w - W_d)/W_d] \times 100 \quad (1)$$

where, W_w and W_d were the weights of the hydrogels at the swelling state and dry state, respectively. All measurements were performed in triplicate.

2.3.6. Hydrolytic degradation

Hydrogel disks of 7 mm diameter and 2 mm thickness were incubated in 48 well-plates with 1 mL of low glucose Dulbecco's Modified Eagle's Medium (DMEM) at 37 °C under agitation at 35 rpm using Stackable Shakers (ThermoScientific MaxQ6000). Culture media was changed every three days and samples were measured gravimetrically after 0 h, 24 h, 3 days, 5 days, 8 days, 10 days, 14 days of incubation by carefully removing any excess water with filter paper and weighing each sample. All experiments were performed in triplicate.

2.3.7. Enzymatic degradation

Enzymatic degradation was performed according to protocols developed for tissue dissociation [50] using Collagenase NBTM (SERVA Electrophoresis GmbH). Briefly, 8.1 U/mL Clostridium histolyticum collagenase was dissolved in Hank's Balanced Salt Solution (HBSS) with 0.169 U/mL neutral protease from Clostridium histolyticum and 2 mM $CaCl_2$, in order to obtain a final collagenase dose of 21 U/g collagenase and 0.43 U/g neutral protease to degrade each CAF sample. Samples were incubated at 37 °C and visualized after 15 min, 30 min, 1 h, 2 h and 3 h. Samples immersed in PBS were used as a negative control. Each test was performed in triplicate.

2.3.8. Rheology analysis

Rheological characterization was performed using a Kinexus Rotational Rheometer (Malvern Instruments Ltd., UK) with 20 mm diameter serrated plates. A special solvent trap system was used to prevent dehydration of the sample during the tests. To identify the linear viscoelastic region (LVR), oscillatory strain sweep tests were applied between 0.01% and 100%. Frequency sweep tests (0.001–10 Hz) were performed at a strain of 0.1% which was within LVR, to study how the elastic modulus (G′), viscous modulus (G″) and viscosity (η) changed with frequency. All tests were done at physiological temperature (37 °C). At least three replicates were used for each test.

2.3.9. Cytocompatibility tests

Cells were cultured at 37 °C and 5% CO2 in a humidified incubator using DMEM™ (Dulbecco's Modified Eagle Medium) basal medium, with high-glucose DMEM™ (Gibco) used for the L929 murine fibroblasts and MIN6 pancreatic beta cells, and low-glucose for the human TERT (Y201) human mesenchymal stem cells. In all cases the basal media was supplemented with 10% FBS, 1% penicillin-streptomycin, with the MIN6 culture medium also supplemented with 25 mM HEPES and 70 μM beta-mercaptoethanol. The hydrogel substrates were placed into Millicell® 24-well culture plates, with different cell populations then seeded dependent on the cell type: 2×10^3 L929 cells per well; 1.6×10^5 MIN6 cells per well; and 5×10^3 Y201 cells per well. In each case the positive control was the same number of cells seeded on tissue culture plastic, and gels without cells were used as the negative control.

2.3.9.1. DNA quantification. Cellular viability was quantified by measuring the DNA content of cells seeded on the hydrogels using the Quanti-iTTM Picogreen® dsDNA assay kit. DNase/RNase-free water was added to each sample and samples were freeze-thawed three times to ensure the complete lysis of the cells. 100 μL of the lysates and 100 μL of the PicoGreen solution (prepared according to the manufacturer's protocol) were added to each well of a 96-well plate. Fluorescence was measured at 480 nm excitation and 520 nm emission using a FLUOstar OPTIMA microplate reader. A standard curve of DNA was produced using known concentrations of lambda DNA (Invitrogen).

2.3.9.2. Live-dead staining assay. L3224 Live/Dead assay (Life Technologies, UK), in brief, 4 μM ethidium homodimer-1 and 10 μM calcein in PBS were incubated in the dark with the cell-seeded CAF samples for 30 min at 37 °C. Samples were imaged immediately using a Nikon A1R inverted confocal microscope. Stained areas were quantified using ImageJ software (National Institutes of Health, USA).

2.3.9.3. Metabolic activity. Quantified by normalizing results from the PrestoBlue™ assay (Invitrogen, UK) to the corresponding DNA content measured with PicoGreen™, as described above. Culture medium was aspirated and samples were washed with pre-warmed PBS at 37 °C. 10% PrestoBlue™ working solution in culture medium was transferred to wells of a 96 well plate. Samples were incubated at 37 °C, 5% CO_2 for the following durations: 1.5 h for L929, 2 h for Y201 hMSCs and 24 h for MIN6. 100 μL of the PrestoBlue™ solution from each well was assessed in triplicate with the fluorescence measured at 560 nm excitation and 590 nm emission.

2.3.9.4. Cellular morphology analysis. The morphology of the cells was observed by staining their cytoskeleton using rhodamine-phalloidin and the nucleus observed using DAPI. After the culture period, samples were fixed in 4% paraformaldehyde for 15 min and washed three times with PBS. Cells were permeabilised using 0.1% v/v Tween20® in PBS for 5 min. Rhodamine-phalloidin was prepared using 1:100 dilutions of phalloidin-tetramethylrhodamine B isothiocyanate (P1951) in 1% v/v Tween20® for 30 min. Residue of phalloidin-rhodamine was removed by washing samples with 1% v/v Tween20® solution. Samples were immersed in DAPI solution (1 mg/mL) and were imaged using a Nikon A1R inverted confocal microscope.

2.4. Statistical analysis

Data was presented as mean values, standard deviations and/or standard error. Mean values were calculated from three independent experiments of triplicates by group. Statistical analysis was performed by two-way ANOVA followed by Bonferroni Post-hoc tests in GraphPad Prism™ 6 software using a level of significance of $p < 0.1$ (*), $p < 0.05$ (**), $p < 0.001$ (***) and $p < 0.0001$(****).

3. Results

3.1. Synthesis and physic-chemical characterization of CAF hydrogels

The main IR peaks attributed to fibrin and collagen were detected in all three formulations (Fig. 1). These bands are mostly associated with the amide groups present in both proteins. The bands for collagen and fibrin shown in Fig. 1.A and B, are mainly at ~1652–1638 cm^{-1} (amide I, C═O stretching), ~1552–1540 cm^{-1} (amide II, N−H bending), ~1333–1312 cm^{-1} and ~1240–1224 cm^{-1} (amide III, N−H bending and C−N stretching). These bands (amide I, II and III) were detected in all three spectra of hydrogels and reported in Fig. 1.B. Spectral changes on amide I and II were identified for hydrogels prepared with different collagen concentrations. C═O stretching of amide I and N−H bending of amide II in hydrogels were slightly shifted to lower frequencies by increasing collagen concentrations. N−H and C−N bending of amide III for the three hydrogels peaks was found within the range of both the characteristic collagen and fibrin bands. The C═O symmetric stretching of COO− at 1418 cm^{-1} was found in all three hydrogels, as well as a sharp peak at 1025 cm^{-1} related to CO, COC and CC stretching. The characteristic peaks of alginate, C═O symmetric stretching of COO− were found in all hydrogels and shifted to lower frequencies by increasing collagen concentration. The spectrum for the 2.5% w/v collagen was closer to the characteristic peak for C═O, indicating symmetric stretching of COO− of collagen.

SEM and image analysis showed pore sizes in the range of 40–120 μm for all three hydrogels (Fig. 2.A). As the collagen concentration increased, more closed and less interconnected pores were observed. TEM (Fig. 2.B) showed a dense protein network was formed in all samples, with freely organized fibrillary structures. These structures became more compact and dense with increasing collagen concentration. Interestingly, the thickest fibres were observed in 1%

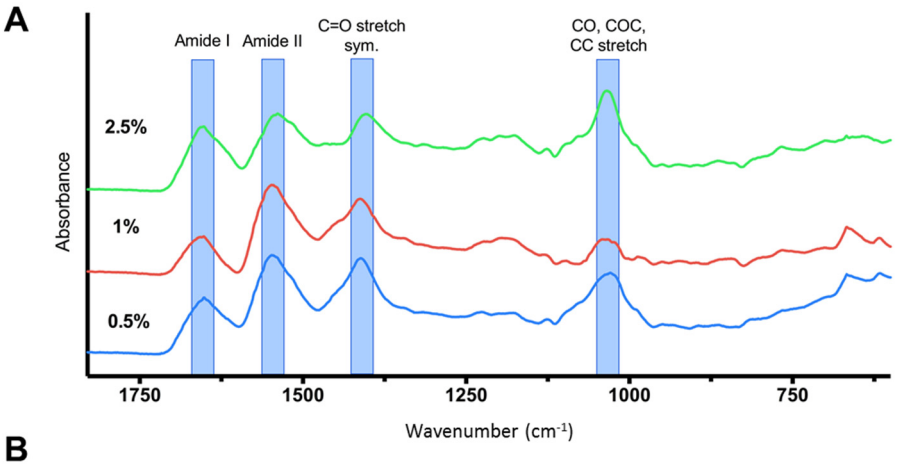

B

Chemical bonds [cm^{-1}]	Collagen	Fibrin	Alginate	0.5% Col.	1% Col.	2.5% Col.
C=O stretching (Amide I)	1652	1638	-	1634	1634	1627
NH bending (Amide II)	1552	1540	-	1548	1547	1539
C=O stretching of COO-	1404	1394	1418	1414	1409	1405
NH bending (Amide III)	1333	1312	-	1317	1316	1312
CN stretching (Amide III)	1240	1224	-	1235	1235	1233
CO stretching	1080	1077	-	1077	1075	1078

Fig. 1. FTIR of synthesized CAF hydrogels produced with different collagen concentrations: A. IR absorbance spectra, and B. IR characteristic peaks.

collagen samples.

The gelation time, swelling, stability and hydrolytic/enzymatic degradation properties of the CAF hydrogels are summarized in Fig. 3. Gelation time defined as the sol-gel transition of the 0.5%, 1% and 2.5% collagen hydrogels was determined by using the "vial tilt" method. All formulations formed self-supporting hydrogels (Fig. 3.A), however the time at which the inverted solution no longer flowed was found dependent of temperature and collagen concentrations. Gelation of hydrogels happened when temperature was increased to 37 °C, and gelation time was reduced as collagen concentration increased ranging from 40 ± 5 min for the 2.5% collagen concentration to 60 ± 10 min for the 0.5% collagen concentration. Once the gel was fully formed, the hydrogel was then stabilized by polymerizing the alginate and fibrinogen components with $CaCl_2$ and thrombin, respectively. The swelling ratios (Fig. 3.B) generally decreased with increasing collagen content, however the differences were not statistically significant. Fig. 3.C demonstrates that hydrogels made with 1% and 2.5% collagen maintained their mass and morphology for 15 days, while the 0.5% collagen hydrogels demonstrated a sharp loss of mass at day 7.

Collagenase-based enzymatic degradation of the three CAF hydrogels was much more rapid than hydrolytic degradation (Fig. 3.D). All hydrogels remained stable when incubated in collagenase solution for

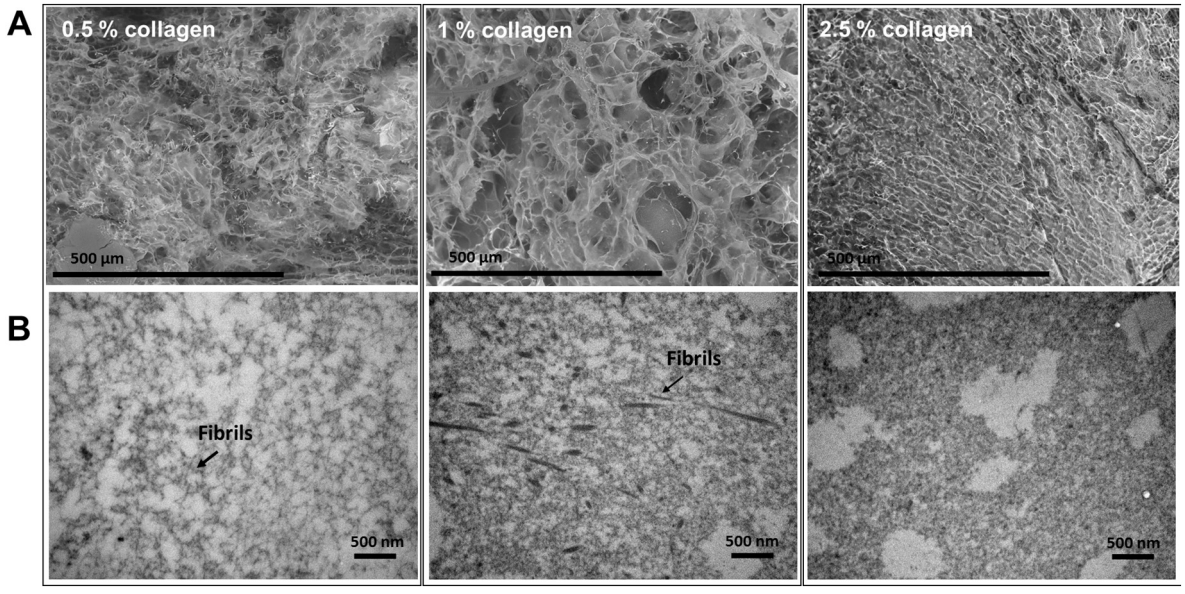

Fig. 2. Microstructure and organization: A. SEM and B.TEM of CAF hydrogel at 0.5% w/v, 1% w/v, and 2.5% w/v collagen concentration.

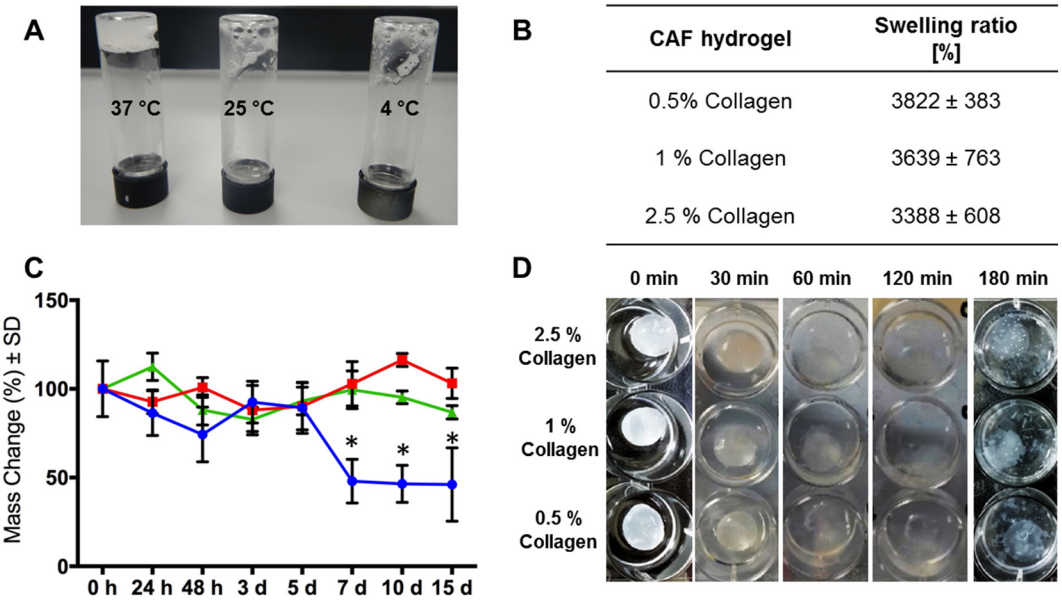

Fig. 3. A. Thermo-responsive CAF hydrogels at 37 °C, B. Rate of hydrogel swelling, C. Hydrolytic degradation (2.5% green, 1% red, 0.5% blue) and, D. Enzymatic degradation with collagenase. Data represent mean values ± SD (n = 3), significance threshold (*p < 0.1) after two-way ANOVA with Bonferroni Post-hoc test relative to initial mass (day 0). (For interpretation of the references to color in this figure legend, the reader is referred to the web version of this article.)

30 min at 37 °C. However, after 30 min, the onset of degradation was observed in the 0.5% collagen hydrogel samples. Degradation was more obvious after one hour in the 1% and 2.5% collagen hydrogel samples, but the morphology of samples was maintained. Following 2 h incubation, all three hydrogels were mostly dissolved. Three hours post-incubation, all hydrogels were completely dissolved in the collagenase solution with residual debris dispersed in the solution. CAF samples incubated in PBS did not exhibit any degradation within the 3-hour test period (data not shown).

Fig. 4 shows the rheological properties of CAF hydrogels. Across all test conditions, the 2.5% collagen formulation was slightly less than twice as stiff as the 1% collagen formulation, which was approximately twice as stiff as the 0.5% collagen formulation. Fig. 4.A shows how the elastic moduli (G′) of samples changed with increasing shear strain (γ*). Elastic moduli for all samples remained stable until the shear strain reached 1%, with moduli of 5 kPa, 2.9 kPa and 1.4 kPa for the 2.5%, 1% and 0.5% collagen formulations, respectively. Beyond this strain, elastic moduli gradually decreased due to breakdown of the internal hydrogel structure. Fig. 4.B–D displays how the elastic moduli (G′), viscous moduli (G″) and viscosity (η*) of different samples change with

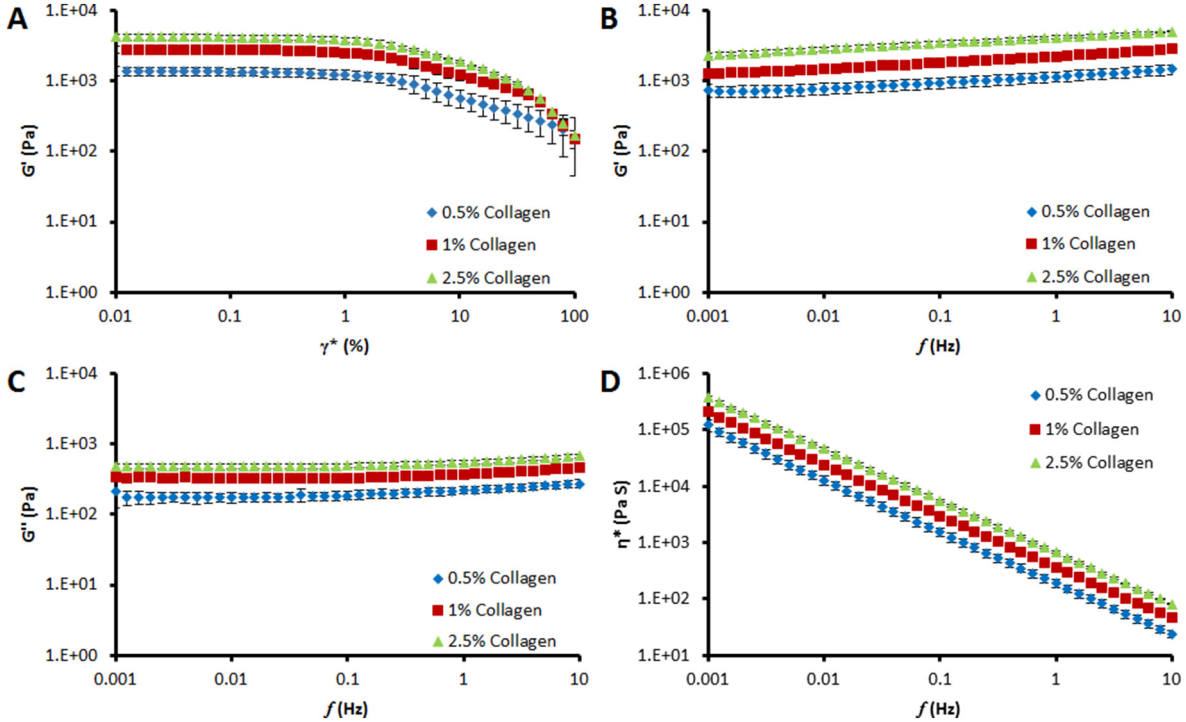

Fig. 4. Dynamic rheological properties of hydrogels: A. Elastic moduli (G′) as a function of shear strain (γ*); B. Elastic moduli as a function of frequency (f); C. Viscous modulus (G″) as a function of frequency, D. Viscosity (η*) as a function of frequency.

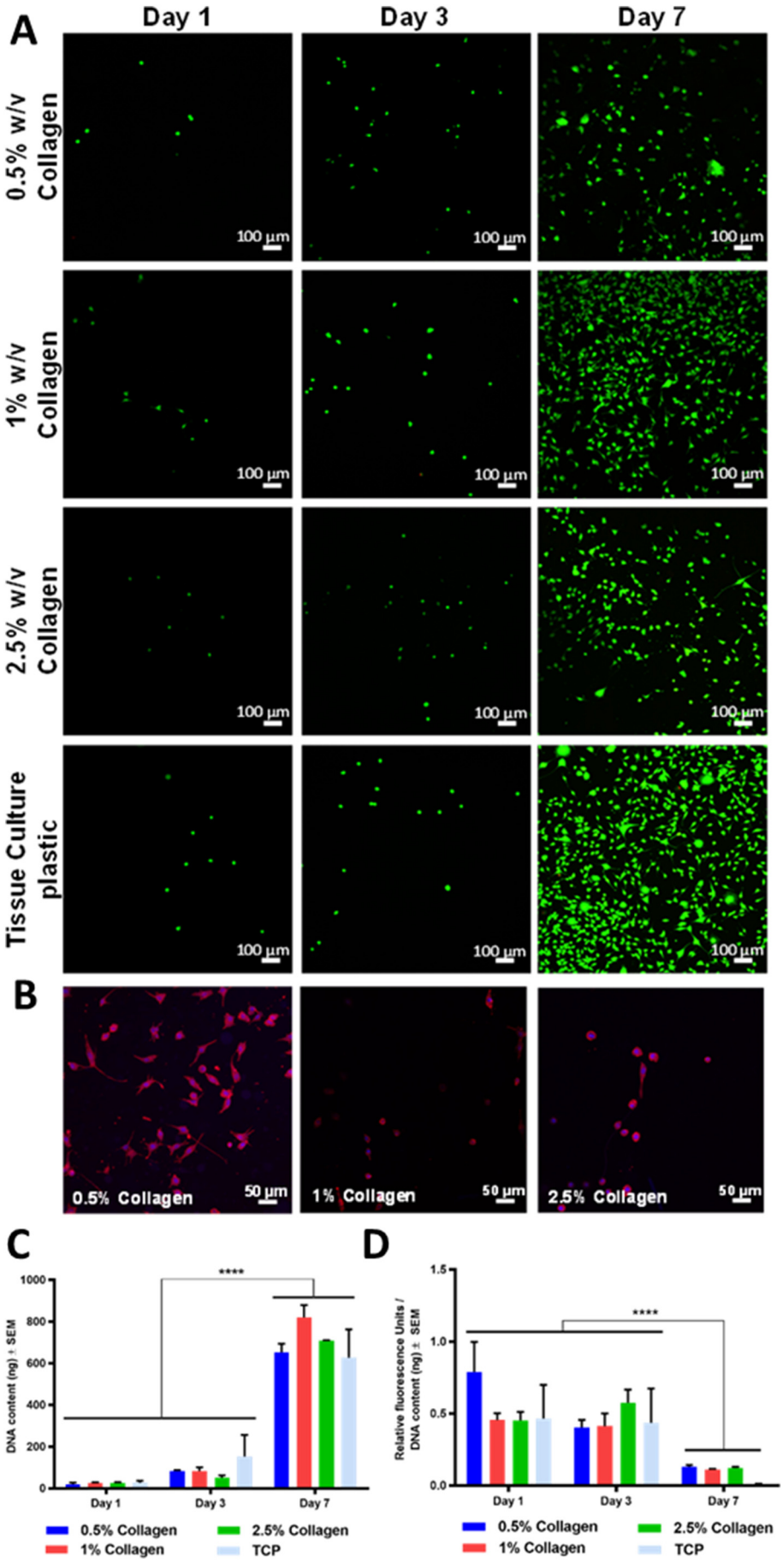

Fig. 5. Cellular behaviour of L929 murine fibroblast cells cultured at 0.5%, 1%, 2.5% w/v collagen hydrogel concentrations and tissue culture plastic (as control). A. Live/Dead cell membrane staining; B. Fibroblastic cell morphology by confocal microscopy after 1 day in culture (Red: phalloidin, Blue: nuclei); C. DNA content as quantification of the total number of viable cells; D. Metabolic activity normalized to DNA content per sample on days 1, 3 and 7 of cell culture on CAF hydrogel surfaces. Data represent mean values ± SEM (n = 3), significance threshold (*$p < 0.1$, **$p < 0.05$, ***$p < 0.001$ and ****$p < 0.0001$) after two-way ANOVA with Bonferroni Post-hoc test relative to each type of sample within and between time points (For interpretation of the references to color in this figure legend, the reader is referred to the web version of this article.)

frequency (f). It can be seen that the elastic moduli (G′) values of all hydrogels gradually increased with frequency; while viscosity (η*) values significantly decrease with frequency. The elastic moduli (G′) are larger than the viscous moduli (G″), indicating that CAF hydrogels are in the solid state, where elastic properties dominate. The viscous moduli (G″) remained almost constant when the frequency was below 0.1 Hz; after which they increased with frequency. All three hydrogel formulations show a similar rate of drop in viscosity as frequency increases.

3.2. Response L929 murine fibroblasts to CAF hydrogels

Live/dead staining (Fig. 5.A) demonstrated that the L929 s were viable with intact cell membrane (green fluorescent cells) and little to no evidence of dead cells (red fluorescent cells) over a 7-day period. No significant differences were observed in cell morphology with changing collagen concentrations (Fig. 5.B). DNA quantification (Fig. 5.C) and normalized Presto Blue reading to DNA content (Fig. 5.D) showed that the cells were proliferating, but there were no significant differences in cell number and proliferation rate on the different substrates within each time point.

3.3. Response of pancreatic MIN6 murine β-cells to CAF hydrogels

Large (50–150 μm) aggregates of MIN6 β-cells were observed after 3 days of culture for all concentrations of collagen (Fig. 6.A). However, higher collagen concentrations led to formation of larger pseudo-islets. Importantly, larger MIN6 clusters also demonstrated higher levels of cell death and necrotic core formation; something observed when clusters outgrow nutrient provision by diffusion. Actin and nuclear cellular staining supported the observations from the Live/Dead analysis of pseudo-islet formation in MIN6 cells (Fig. 6.B). At day 3, actin filament staining illustrated significant cell clustering and limited cell spreading on the surface of the CAF hydrogels. No significant differences in DNA content were observed amongst the MIN6 cells cultured on the CAF substrates. However, a significant increase in DNA content was found at day 3 on 0.5% collagen hydrogels (Fig. 6.C). The DNA content was significantly higher on tissue culture plastic when compared with CAF hydrogels at days 3 and 7. The MIN6 cells had low metabolic activity levels at days 1 and 3, with a significant increase at day 7 (Fig. 6.D). Notably, cells seeded on CAF gels with 0.5% collagen had greater levels of activity than cells on gels made with 1% and 2.5% collagen at day 7, although initial metabolic activity was significantly higher on the 2.5% collagen gel at day 1.

3.4. Response of human mesenchymal stem cells to CAF hydrogels

Y201 hMSCs were viable when cultured on top of the three collagen concentrations of CAF hydrogels (Fig. 7.A). The presence of elongated cells was found to correlate with increasing collagen content in hydrogels on day 1 (Fig. 7.B). No significant differences in DNA content were observed amongst the Y201 cells cultured on the CAF substrates (Fig. 7.C). Greater cell proliferation was found in all CAF hydrogels following 7 days of culture. Cells cultured on the CAF hydrogel did not show any significant differences in terms of metabolic activity at days 3 and 7, but a significantly higher metabolic activity was detected on the 0.5% collagen hydrogel compared to the other substrates at day 1 (Fig. 7.D). Notably, a significant increase of alkaline phosphatase (ALP) activity was found in 2.5% collagen hydrogels from day 1 to 7 suggesting an enhanced osteogenic potential with high collagen content (Fig. 7.E).

4. Discussion

4.1. Physic-chemical and morphological properties of CAF hydrogels

The most relevant peaks of the three components: collagen, alginate and fibrin were well represented in all the FTIR-ATR spectra of hydrogels with 0.5%, 1% and 2.5% collagen (Fig. 1). Downshifts of typical bands under higher collagen concentrations are attributed to the gradual weakening of specific molecular interactions, such as hydrogen bonding and dipole–dipole interactions [51]. Hydrogen bonding in proteins such as collagen is closely related to interactions between water and the C═O and N−H groups of the protein backbone [52], these interactions lower the amide I and amide II intensities [53]. This effect is closely related to the hydration level of the protein within the hydrogel. The swelling results showed that hydrogel hydration tends to decrease with increasing collagen content. This supports the IR results, which indicate a weakening of hydrogen bonds (established by H_2O molecule interactions with neighbouring molecules) with increasing collagen concentration. Further analysis, such as nuclear magnetic resonance (NMR) spectroscopy and X-ray photoelectron spectroscopy (XPS), would support a deeper understanding of the hydrogel chemical structure. The hydrolytic degradation results show that weakening hydrogen bonds may impact the hydration degree within the hydrogel lattice as well as the stability of the hydrogel under physiological conditions. Hydrogels formulated with higher collagen concentrations were able to maintain their morphology and mass for 15 days, while 0.5% collagen hydrogels lost about half of their initial mass after 7 days. With increasing collagen content within CAF hydrogel formulations: 1) the hydrogen bonds between water and the different components of the gel are weakened; 2) the capacity to retain water within the lattice decreases; and 3) the hydrogel lattice is stabilized by reducing the presence of water molecules to break down bonds of the three components under physiological conditions.

The gelation time was affected by the amount of collagen protein since higher concentrations of collagen would favour the kinetic process of aggregating collagen molecules at physiological conditions. The average gelation time was shorter with increasing collagen content within the hydrogel. This was confirmed by the TEM data as hydrogels at higher collagen concentrations exhibited a more dense and organized structure with formation of nano-fibrils [54,55]. CAF hydrogels were found to be fully degraded and fragmented after 2 h of incubation in collagenase solution, without significant differences between the formulations. However, the 0.5% collagen hydrogel was the first to visibly degrade and dissolve, which is consistent with collagen playing a key role in the structural integrity of CAF hydrogels. A quicker enzymatic degradation through routine procedure for cells isolation represents an advantage in clinical transplantation, i.e. as islets carrier in diabetic therapeutic applications.

CAF hydrogels exhibited a porous structure with pore sizes in the range of 40–120 μm, and the homogeneity of the micro-structure was shown to decrease with an increasing concentration of collagen. Freeze-dried hydrogels with 0.5% and 1% collagen showed a more open and interconnected porous structure than at 2.5% collagen. The closed micro-pores observed in the freeze-dried hydrogels at the 2.5% collagen concentration may introduce limitations on nutrient transfer and metabolite diffusion within the gels, and may inhibit the formation of neovascular structures following implantation [56,57]. Therefore, depending on the collagen concentration, the CAF hydrogel may be able to provide a suitable biomaterial for cell culture and tissue engineering applications; since pore sizes in the 10–150 μm range are normally identified in scaffolds intended as support for growing and proliferating cells [58].

The elastic and viscous moduli for all hydrogels showed behaviour typical of viscoelastic materials [59]. A positive correlation was observed between increasing collagen content and increasing values of both G′ and G″, with the concentration of collagen in the hydrogel not

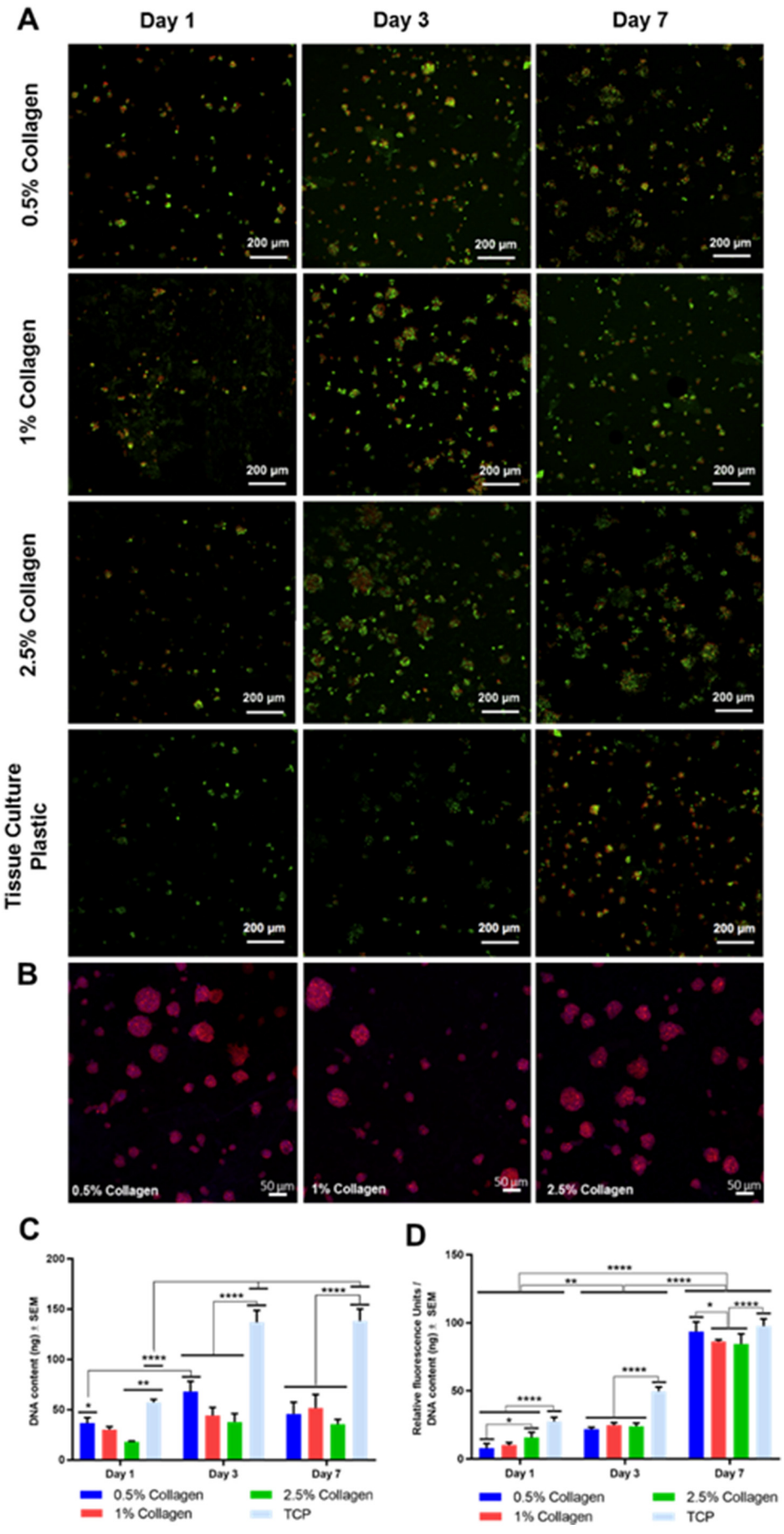

Fig. 6. MIN6 β-cell behaviour on the surface of CAF hydrogels at different collagen concentrations (0.5%, 1%, 2.5% w/v) and tissue culture plastic as control: A. Live/Dead cell membrane staining; B. Confocal microscopy of MIN6 β-cells after 1 day in culture (Red: phalloidin, Blue: nuclei); C. Cellular DNA content as measurement of viable cells per sample; D. Metabolic activity normalized to DNA content per sample on days 1, 3 and 7 of cell culture. Data represent mean values ± SEM (n = 3), significance threshold (*p < 0.1, **p < 0.05, ***p < 0.001 and ****p < 0.0001) after two-way ANOVA with Bonferroni Post-hoc test relative to each type of sample within and between time points. (For interpretation of the references to color in this figure legend, the reader is referred to the web version of this article.)

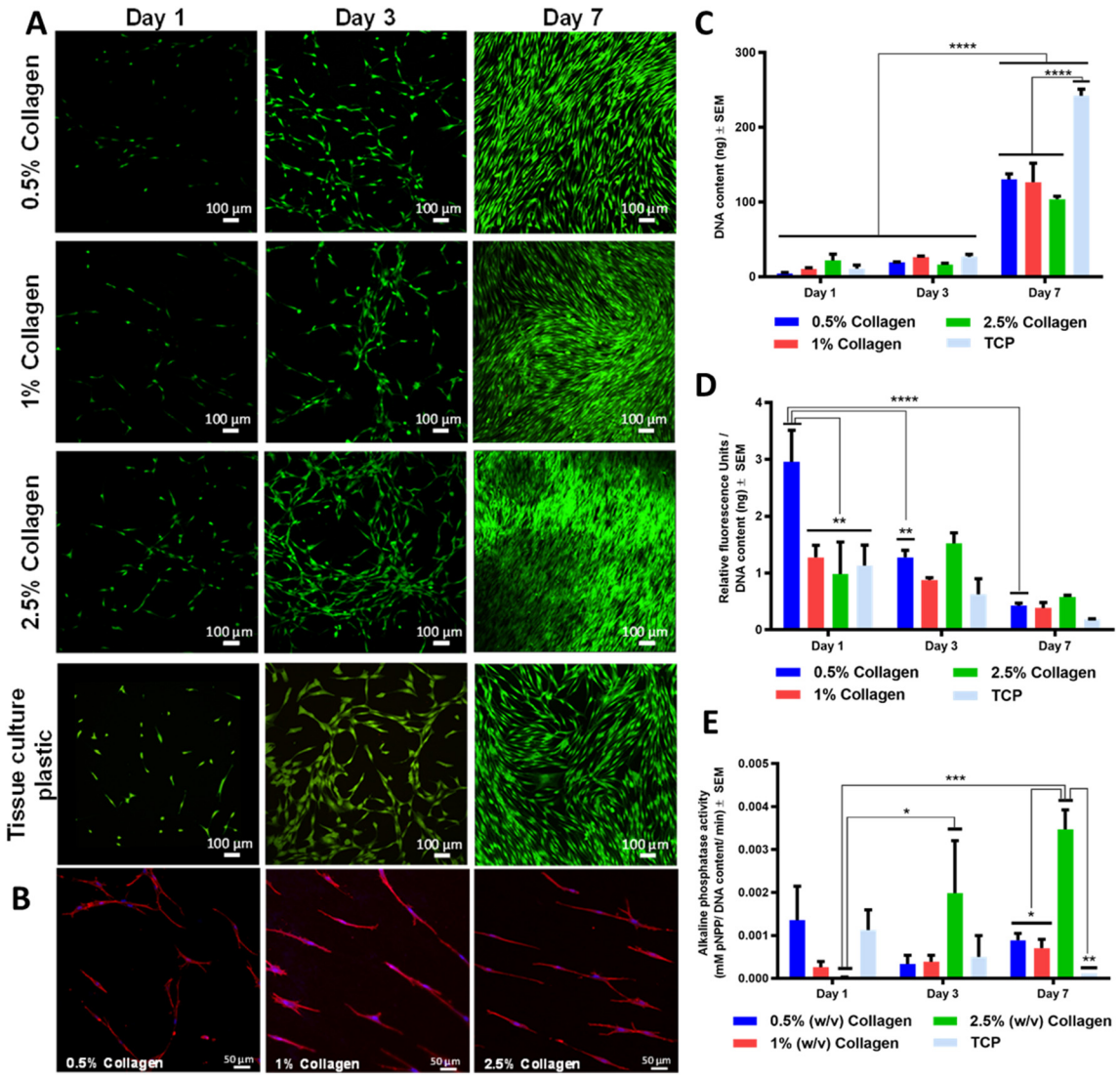

Fig. 7. Cellular behaviour of Y201 cells cultured on CAF hydrogels surfaces at 0.5%, 1%, 2.5% w/v collagen concentrations and tissue culture plastic (as control): A. Live/Dead cell membrane staining; B. Confocal images Y201 cell morphology after 1 day in culture (Red: phalloidin, Blue: nuclei); C. Cellular DNA content as measurement of total viable cells; D. Metabolic activity normalized to DNA content; E. Alkaline Phosphatase Activity (ALP) normalized to DNA content after 1, 3 and 7 days in culture. Data represent mean values ± SEM (n = 3), significance threshold (*p < 0.1, **p < 0.05, ***p < 0.001 and ****p < 0.0001) after two-way ANOVA with Bonferroni Post-hoc test relative to each type of sample within and between time points. (For interpretation of the references to color in this figure legend, the reader is referred to the web version of this article.)

affecting the critical strain. All CAF hydrogel formulations were observed to maintain stable values of G′ and G″, which defined their linear viscoelastic regime (LVR) up to almost 1% of deformation. For comparison, type-I collagen gel has G′ of the order of 10 kPa, alginate gel has G′ of the order of 100 kPa, and the elastic modulus of soft tissues is in the range 0.1 to 1000 kPa [15,59]. The three CAF hydrogels have values ranging from 0.5 to 5 kPa, positioning them at the lower end of the range for soft tissues, similar to collagen gels. This range is relevant to many human tissues; for example bulk human pancreatic tissue has similar values of G′ and G″ to the CAF gels [59].

4.2. Biological response

Murine fibroblast L929 cells have been widely utilised for cytotoxity and cytocompatibility assays with a variety of materials [60,61]. From this study, it was observed that the L929 cells seeded on top of the gels remained viable with no indication of cell death throughout the culture duration. The different concentrations of collagen had no influence on the viability, proliferation rate, metabolic activity and morphology of this cell line.

Research aimed at understanding insulin secretion and β-cell dysfunction in diabetes commonly uses rodent models; since glucose homeostasis in these animals is similar to humans [62]. MIN6 β-cells derived from a mouse pancreatic cancer line have the capacity to form three-dimensional clusters, known as pseudo-islets, which mimic the structure and function of primary islet β-cells [63,64]. Large (50–150 µm) aggregates of MIN6 β-cells were observed after day 3 for all concentrations of collagen investigated; indicating formation of pseudo-islets. Higher collagen concentrations led to larger pseudo-islets and increased cell death, as shown by Live/Dead staining. Cell death of MIN6 β-cells has been found to be upregulated in islet-like spheroid structures due to the lack of active vascular nutrient delivery into the spheroids [65]. The formation of larger pseudo-islets in CAF hydrogels with higher collagen concentrations may result from the key role that extracellular matrix (ECM) proteins play in regulating β-cell organization, survival and insulin secretion [66]. Formulated CAF hydrogel represents a unique platform for tailoring biomimetic microenvironments to enhance pancreatic β-cells response for treating diabetes type I.

Table 1
Properties and clinical applications of CAF hydrogels with varying collagen content (Low is indicated as +, medium as ++ and high as +++).

Type of hydrogel	Stability [days]	Ease of use	Gelation time [min]	Swelling ratio	Mechanical properties	Porosity	Cytocompatibility			Potential clinical applications
							L929	hMSCs	β-cells	
0.5% Col	+	++	+++	+++	+	+++	+++	+++++	++	Bioprocessing and short-time cell delivery, bioink
1% Col	++	+++	++	+++	++	++	+++	++	+++	Soft tissues (i.e. pancreas and Islets encapsulation, liver, skin, etc.)
2.5% Col	+++	+	++	+++	+++	++	+++	+++	+++	Cartilage and osteochondral, soft bone, periodontal applications

Pseudo-islet formation has been linked to reduced proliferation due to increased expression of cyclin-dependent kinase inhibitors and down regulation of ki67 [67]. Here, proliferation was not quantified explicitly, but DNA content was similar for most collagen concentrations. The exceptions were significant increases at day 3 with cells on 0.5% collagen gels and with cells grown on tissue culture plastic. This could be linked to the formation of smaller pseudo-islets on these substrates and higher rates of proliferation. Notably, higher levels of MIN6 metabolic activity were found for 1% and 2.5% collagen hydrogels than the 0.5% collagen hydrogels. Importantly, insulin secretion in transformed β-cells is not influenced by reduction of proliferation [68]. The results of this study suggest that CAF hydrogels promote pseudo-islet formation and metabolic activity in MIN6 β-cells. Furthermore, hydrogels with higher concentrations of collagen allow for larger islets to grow and increase the metabolic activity of the pancreatic cells. This could be facilitated via up-regulation of cell adhesion molecules and ECM components in gels containing more collagen.

Y201 hMSCs cultured on the CAF hydrogels with collagen 0.5% and 1% w/v proliferated significantly after day 3; but cells cultured on hydrogels with 2.5% w/v collagen showed no significant increase in proliferation over the same period. However, Y201 cells seeded on the top of 2.5% w/v collagen CAF hydrogel produced a significant increase in ALP activity after day 3. A lack of cellular proliferation accompanied by an increase of ALP activity is indicative of osteoblastic differentiation [69–71]. The enhanced osteogenic potential of Y201 cells on CAF hydrogels with 2.5% collagen could be due to the high collagen concentration and higher material stiffness that have been previously linked to osteogenic differentiation [72–74]. A common phenomenon observed for both the L929 and Y201 cell lines seeded on top of the CAF hydrogels was a decrease in metabolic activity over the course of the experiment, while cells were still proliferating. This is likely to be the result of high cell confluency; since results were similar to those for the tissue culture plastic control.

The formulated tri-component CAF hydrogel has been found to have a useful range of physical-chemical, mechanical and biological properties for applications in tissue engineering, cell-therapy, development of in-vitro models, cell culture and bioprocessing. A comparison between the CAF hydrogels with potential applications is summarized in Table 1.

The similarities in terms of viscoelastic properties found between CAF hydrogels and native soft tissues such as the pancreas and liver, offers significant potential for this hydrogel to be used as a biomaterial for soft tissue engineering applications, cell-therapy and delivery, cell culture and bioprocessing for regenerative medicine. For bioprocessing applications, CAF hydrogels with 0.5% to 1% collagen content may represent a promising material due to the low viscosity and soft post-assembly matrix. Both the 0.5% and 1% collagen CAF hydrogels exhibit a final homogeneous structure which mimics the mechanical properties of a variety of soft tissues as verified by rheological studies, while still providing interconnected pores suitable for diffusion and exchange of nutrients and oxygen which may facilitate neovascularization within 3D constructs [75–77]. In contrast, the 2.5% collagen CAF hydrogels offer potential in applications where stiffer matrices are required in order to guarantee greater mechanical properties and scaffold stability over time. As the 2.5% collagen CAF hydrogel appeared to promote osteogenic activity of Y201 cells, they may be considered in combination with structural biomaterials for engineering musculoskeletal tissues.

5. Conclusions

A new thermo-responsive hydrogel based on collagen, alginate, and fibrin has been synthesized and characterized. CAF hydrogels gel rapidly at physiological conditions, allowing material delivery in the fluid state at room temperature and subsequent crosslinking at 37 °C. CAF hydrogels can remain stable for up to 15 days; exhibiting swelling between 3000 and 4000%, mechanically similar to native soft tissues with elastic modulus between 0.1 and 1000 kPa, and pore sizes between 40 and 120 μm. Cytocompatibility was demonstrated for three cell lines: L929 fibroblasts exhibited similar viability and enhanced proliferation to those cultured on traditional tissue culture plastic; hMSCs showed enhanced osteogenic potential at higher concentrations of collagen; and MIN6 β-cells were able to form larger pseudo-islet clusters with a higher metabolic activity as collagen content increased. CAF hydrogels offer a tuneable microenvironment that supports cell survival and function for cell culture applications, and has potential for cell-based regenerative medicine therapies. Further investigation of this material will consider specific applications such as endocrine pancreas tissue engineering and musculoskeletal applications.

Acknowledgements

The authors would like to thank Kath White and Tracey Davis at Electron Microscopy Research Services (Newcastle University) and Alex Laude at Bioimaging Unit (Newcastle University) for their kind support. The author would like to thanks also Prof. Paul Genever (York University) for providing the h-TERT Y201 MSCs used in this work, Ms. Cecilia Olivieri for her support on the initial research activities on the hydrogel formulation; and Prof Jim Shaw, Dr. Catherine Arden and Ms. Minna Honkanen-Scott for provision of MIN6 β-cells and collagenase for enzymatic digestions tests. The research has been financially supported by the EPSRC Re-distributed Manufacturing in Healthcare Network (RiHN; EP/M017559/1), the EPSRC Centre for Innovative Manufacture in Medical Devices (MeDe Innovation; EP/K029592/1) and the Arthritis Research UK Tissue Engineering Centre (Award 19429).

References

[1] S.W. Crowder, V. Leonardo, T. Whittaker, P. Papathanasiou, M.M. Stevens, Cell Stem Cell 18 (2016) 39–52.
[2] J.L. Drury, D.J. Mooney, Biomaterials 24 (2003) 4337–4351.
[3] J. Kopeček, Biomaterials 28 (2007) 5185–5192.
[4] F. Brandl, F. Sommer, A. Goepferich, Biomaterials 28 (2007) 134–146.
[5] D. Seliktar, Science 336 (2012) 1124–1128.
[6] G.M. Beattie, A.M.P. Montgomery, A.D. Lopez, E. Hao, B. Perez, M.L. Just, J.R.T. Lakey, M.E. Hart, A. Hayek, Diabetes 51 (2002) 3435–3439.
[7] J.W. Weisel, R.I. Litvinov, Blood 121 (2013) 1712–1719.

[8] U. Hersel, C. Dahmen, H. Kessler, Biomaterials 24 (2003) 4385–4415.
[9] M.P. Lutolf, G.P. Raeber, A.H. Zisch, N. Tirelli, J.A. Hubbell, Adv. Mater. 15 (2003) 888–892.
[10] S.V. Murphy, A. Skardal, A. Atala, J. Biomed. Mater. Res. A 101A (2013) 272–284.
[11] G.D. Nicodemus, S.J. Bryant, Tissue Eng. B Rev. 14 (2008) 149–165.
[12] J.J. Schmidt, J. Rowley, H.J. Kong, J. Biomed. Mater. Res. A 87 (2008) 1113–1122.
[13] N. Gjorevski, A. Ranga, M.P. Lutolf, Development 141 (2014) 1794–1804.
[14] Y. Tabata, M.P. Lutolf, Sci. Rep. 7 (2017) 44711.
[15] E.E. Antoine, P.P. Vlachos, M.N. Rylander, PLoS One 10 (2015) e0122500.
[16] C. Dong, Y. Lv, Polymer 8 (2016) 42.
[17] W. Friess, Eur. J. Pharm. Biopharm. 45 (1998) 113–136.
[18] A.M. Ferreira, P. Gentile, V. Chiono, G. Ciardelli, Acta Biomater. 8 (2012) 3191–3200.
[19] A.D. Augst, H.J. Kong, D.J. Mooney, Macromol. Biosci. 6 (2006) 623–633.
[20] J.A. Rowley, G. Madlambayan, D.J. Mooney, Biomaterials 20 (1999) 45–53.
[21] P.A. Janmey, J.P. Winer, J.W. Weisel, J. R. Soc. Interface 6 (2009) 1–10.
[22] H. Zhao, L. Ma, J. Zhou, Z. Mao, C. Gao, J. Shen, Biomed. Mater. 3 (2007) (015001).
[23] P.X. Ma, Adv. Drug Deliv. Rev. 60 (2008) 184–198.
[24] R. Jin, P.J. Dijkstra, Hydrogels for tissue engineering applications, Biomedical applications of hydrogels handbook, Springer, 2010, pp. 203–225.
[25] M. Xu, X. Wang, Y. Yan, R. Yao, Y. Ge, Biomaterials 31 (2010) 3868–3877.
[26] Y. Xu, X. Wang, Biotechnol. Bioeng. 112 (2015) 1683–1695.
[27] J. Grzesiak, J. Kolankowski, K. Marycz, J. Biomater. Tissue Eng. 5 (2015) 703–710.
[28] H. Zhou, H.H.K. Xu, Biomaterials 32 (2011) 7503–7513.
[29] K. Ma, A.L. Titan, M. Stafford, C. Hua Zheng, M.E. Levenston, Acta Biomater. 8 (2012) 3754–3764.
[30] I.R. Brito, G.M. Silva, A.D. Sales, C.H. Lobo, G.Q. Rodrigues, R.F. Sousa, A.A.A. Moura, C.E.M. Calderón, M. Bertolini, C.C. Campello, Reprod. Domest. Anim. 51 (2016) 997–1009.
[31] S. Sakai, S. Yamaguchi, T. Takei, K. Kawakami, Biomacromolecules 9 (2008) 2036–2041.
[32] B. Balakrishnan, N. Joshi, A. Jayakrishnan, R. Banerjee, Acta Biomater. 10 (2014) 3650–3663.
[33] B. Duan, L.A. Hockaday, K.H. Kang, J.T. Butcher, J. Biomed. Mater. Res. A 101 (2013) 1255–1264.
[34] M.C. Gómez-Guillén, B. Giménez, M.E.A. López-Caballero, M.P. Montero, Food Hydrocoll. 25 (2011) 1813–1827.
[35] N. Davidenko, C.F. Schuster, D.V. Bax, R.W. Farndale, S. Hamaia, S.M. Best, R.E. Cameron, J. Mater. Sci. Mater. Med. 27 (2016) 148.
[36] R.A. Perez, M. Kim, T.-H. Kim, J.-H. Kim, J.H. Lee, J.-H. Park, J.C. Knowles, H.-W. Kim, Tissue Eng. A 20 (2013) 103–114.
[37] B.M. Gillette, J.A. Jensen, B. Tang, G.J. Yang, A. Bazargan-Lari, M. Zhong, S.K. Sia, Nat. Mater. 7 (2008) 636.
[38] L. Zheng, X. Jiang, X. Chen, H. Fan, X. Zhang, Biomed. Mater. 9 (2014) 065004.
[39] C.J. Little, W.M. Kulyk, X. Chen, J. Funct. Biomat. 5 (2014) 197–210.
[40] B. Sayyar, M. Dodd, L. Marquez-Curtis, A. Janowska-Wieczorek, G. Hortelano, Artif. Cells Nanomed. Biotechnol. 42 (2014) 102–109.
[41] C.S. Linsley, B.M. Wu, B. Tawil, J. Biomed. Mater. Res. A 104 (2016) 2945–2953.
[42] M. Bongio, S. Lopa, M. Gilardi, S. Bersini, M. Moretti, Nanomedicine 11 (2016) 1073–1091.
[43] C. Schneider-Barthold, S. Baganz, M. Wilhelmi, T. Scheper, I. Pepelanova, BioNanoMaterials 17 (2016) 3–12.
[44] T. Yuan, L. Zhang, K. Li, H. Fan, Y. Fan, J. Liang, X. Zhang, J Biomed Mater Res B Appl Biomater 102 (2014) 337–344.
[45] X. Xiao, S. Pan, X. Liu, X. Zhu, C.J. Connon, J. Wu, S. Mi, J. Biomed. Mater. Res. A 102 (2014) 1782–1787.
[46] S. Harrington, J. Williams, S. Rawal, K. Ramachandran, L. Stehno-Bittel, Hyaluronic acid/collagen hydrogel as an alternative to alginate for long-term immunoprotected islet transplantation, Tissue Eng. A 23 (19–20) (2017) 1088–1099.
[47] B.N.B. Nguyen, R.A. Moriarty, T. Kamalitdinov, J.M. Etheridge, J.P. Fisher, J. Biomed. Mater. Res. A 105 (2017) 1123–1131.
[48] X. Chen, F. Zhang, X. He, Y. Xu, Z. Yang, L. Chen, S. Zhou, Y. Yang, Z. Zhou, W. Sheng, Injury 44 (2013) 540–549.
[49] S. James, J. Fox, F. Afsari, J. Lee, S. Clough, C. Knight, J. Ashmore, P. Ashton, O. Preham, M. Hoogduijn, Stem Cell Rep. 4 (2015) 1004–1015.
[50] T. Kin, Islet Isolation for Clinical Transplantation, Springer, The Islets of Langerhans, 2010, pp. 683–710.
[51] S.R. Ryu, I. Noda, Y.M. Jung, Am. Lab. 43 (2011) 40–43.
[52] Y. Maréchal, J. Mol. Struct. 648 (2003) 27–47.
[53] A. Barth, Biochim. Biophys. Acta-Bioenergetics 1767 (2007) 1073–1101.
[54] D.F. Holmes, H.K. Graham, J.A. Trotter, K.E. Kadler, Micron 32 (2001) 273–285.
[55] A.S. Wolberg, D.M. Monroe, H.R. Roberts, M. Hoffman, Blood 101 (2003) 3008–3013.
[56] B. Feng, Z. Jinkang, W. Zhen, L. Jianxi, C. Jiang, L. Jian, M. Guolin, D. Xin, Biomed. Mater. 6 (2011) 015007.
[57] A.S. Hoffman, Adv. Drug Deliv. Rev. 64 (2012) 18–23.
[58] N. Annabi, J.W. Nichol, X. Zhong, C. Ji, S. Koshy, A. Khademhosseini, F. Dehghani, Tissue Eng. B Rev. 16 (2010) 371–383.
[59] C. Wex, M. Fröhlich, K. Brandstädter, C. Bruns, A. Stoll, J. Mech. Behav. Biomed. Mater. 41 (2015) 199–207.
[60] K.G. Ozdemir, H. Yılmaz, S. Yılmaz, J Biomed Mater Res B Appl Biomater 90 (2009) 82–86.
[61] M.O. Wang, J.M. Etheridge, J.A. Thompson, C.E. Vorwald, D. Dean, J.P. Fisher, Biomacromolecules 14 (2013) 1321–1329.
[62] S.J. Persaud, C. Arden, P. Bergsten, A.J. Bone, J. Brown, S. Dunmore, M. Harrison, A. Hauge-Evans, C. Kelly, A. King, T. Maffucci, C.E. Marriott, N. McClenaghan, N.G. Morgan, C. Reers, M.A. Russell, M.D. Turner, E. Willoughby, M.Y.G. Younis, Z.L. Zhi, P.M. Jones, Islets 2 (2010) 236–239.
[63] A.C. Hauge-Evans, P.E. Squires, S.J. Persaud, P.M. Jones, Diabetes 48 (1999) 1402–1408.
[64] M.J. Luther, A. Hauge-Evans, K.L.A. Souza, A. Jorns, S. Lenzen, S.J. Persaud, P.M. Jones, Biochem. Biophys. Res. Commun. 343 (2006) 99–104.
[65] M.J. Luther, E. Davies, D. Muller, M. Harrison, A.J. Bone, S.J. Persaud, P.M. Jones, Am. J. Physiol.-Endocrinol. Metab. 288 (2005) E502–E509.
[66] K.M. Lee, G.S. Jung, J.K. Park, S.K. Choi, W.B. Jeon, Acta Biomater. 9 (2013) 5600–5608.
[67] A.D. Green, S. Vasu, P.R. Flatt, Exp. Cell Res. 344 (2016) 201–209.
[68] C. Reers, A.C. Hauge-Evans, N.G. Morgan, A. Willcox, S.J. Persaud, P.M. Jones, Islets 3 (2011) 80–88.
[69] D. Baksh, R. Yao, R.S. Tuan, Stem Cells 25 (2007) 1384–1392.
[70] A. Uccelli, L. Moretta, V. Pistoia, Nat. Rev. Immunol. 8 (2008) 726–736.
[71] G. Subramanian, C. Bialorucki, E. Yildirim-Ayan, Mater. Sci. Eng. C 51 (2015) 16–27.
[72] R.M. Salasznyk, W.A. Williams, A. Boskey, A. Batorsky, G.E. Plopper, Biomed. Res. Int. 2004 (2004) 24–34.
[73] W. Zhao, X. Li, X. Liu, N. Zhang, X. Wen, Mater. Sci. Eng. C 40 (2014) 316–323.
[74] C. Linsley, B. Wu, B. Tawil, Tissue Eng. A 19 (2013) 1416–1423.
[75] A. Skardal, A. Atala, Ann. Biomed. Eng. 43 (2015) 730–746.
[76] R. Landers, A. Pfister, U. Hübner, H. John, R. Schmelzeisen, R. Mülhaupt, J. Mater. Sci. 37 (2002) 3107–3116.
[77] T. Courtney, M.S. Sacks, J. Stankus, J. Guan, W.R. Wagner, Biomaterials 27 (2006) 3631–3638.